IOP Conf. Series: Journal of Physics: Conf. Series **1461** (2020) 012173 doi:10.1088/1742-6596/1461/1/012173

Compact Metamaterial-based Coil Element for Combined ^{1}H/^{23}Na MRI at 7 T

Jan Taro Svejda, Andreas Rennings, Daniel Erni

General and Theoretical Electrical Engineering (ATE), Faculty of Engineering, University of Duisburg-Essen, and CENIDE – Center for Nanointegration Duisburg-Essen, D-47048 Duisburg, Germany

E-mail: jan.svejda@uni-due.de, andre.rennings@uni-due.de, daniel.erni@uni-due.de

Abstract. High static magnetic flux densities in the field of magnetic resonance imaging (MRI) allow X-nuclei-based imaging and spectroscopy as well as the utilization of electromagnetic metamaterials. A compact dual-tuned coil element based on a metamaterial transmission line which achieves a quarter-wave resonance at the two distinct operating frequencies of the hydrogen and sodium nuclei is presented. In addition, first combined ^{1}H/^{23}Na MRI measurement results from a structured phantom are shown and discussed.

1. Introduction

The utilization of nuclei other than hydrogen (^{1}H) – the X-nuclei – for MRI and magnetic resonance spectroscopy (MRS) purposes requires additional hardware components such as dual-tuned RF-coils as well as a high background flux density to achieve a usable signal-to-noise-ratio (SNR) due to the lower abundances of X-nuclei in the human body by orders of magnitude compared to ^{1}H. However, the images or data retrieved by X-nuclei offer complementary diagnostic insights to those obtained with the ^{1}H nuclei. It is e.g. possible to rate the health of tissues via the concentration of sodium (^{23}Na) or to visualize metabolites by utilizing the phosphorus (^{31}P) nuclei [1, 2]. For the purpose of combined ^{1}H/^{23}Na MRI a dual-tuned coil element (or antenna) based on a composite right-/left-handed (CRLH) [3] metamaterial transmission line (TL) is presented. The special dispersion characteristic is used to achieve a quarter-wave resonance at both operating frequencies of 78.8 MHz for the ^{23}Na nuclei and 298 MHz for the ^{1}H nuclei in a background magnetic flux density of 7 T and generates thereby a congeneric $\boldsymbol{B}_1$-field distribution which simplifies the comparability of the retrieved MR-images. Due to this operating behavior the element is named congeneric dual-resonant antenna (CDRA) [4].

2. Utilized metamaterial transmission line

In order to achieve the desired dispersion characteristic for a quarter-wave resonance at two distinct frequencies a metamaterial TL consisting of three CRLH unit cells as shown in Fig. 1 are proposed, each providing a 30° phase shift at 78.8 MHz and 298 MHz, respectively. The unit cell is basically a microstrip line (MSL) with additional series capacitors in form of metal-insulator-metal (MIM) assemblies and a shunt inductor represented by a short-circuited coaxial stub line. The corresponding equivalent circuit (EC) is given in Fig. 2, where the parameters

IOP Conf. Series: Journal of Physics: Conf. Series **1461** (2020) 012173 doi:10.1088/1742-6596/1461/1/012173

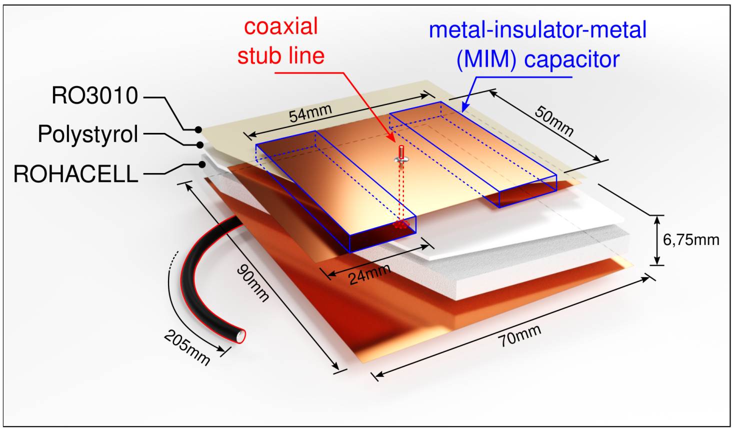

Figure 1. Construction of a single unit cell where a basis microstrip line is augmented with series MIM capacitors and a coaxial stub line terminated with a short circuit to form a CRLH TL.

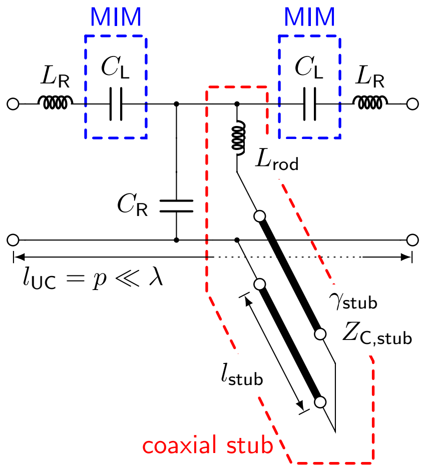

Figure 2. Equivalent circuit of the unit cell structure shown in Fig. 1.

of the lumped elements can be analytically predicted in a first attempt. To obtain the EC parameters of the MSL with finite ground plane the capacitance and inductance values per unit length given in [4] are multiplied with the unit cell length p. The coaxial stub line shows in case of the given design an inductive input impedance at the lower operating frequency, whereas it presents capacitive behavior at the higher frequency. This enables a left-handed (LH) propagation at the low frequency on the one hand and an increase of the phase constant β in the right-handed (RH) range on the other hand (cf. Fig. 3).

To form geometrically compact series capacitors the Rogers substrate material RO3010 with a high relative permittivity of 11.2 and a thickness of 250 µm is utilized. Due to the fragility of the material, it was applied to a polystyrene carrier with a thickness of 1 mm. To maintain a constant height of the MSL a foam spacing layer ROHACELL 31HF with almost air like properties is used.

Fig. 3 gives the dispersion diagram associated with this unit cell and the desired operating points with the principle current distributions along the cable. On one hand the dispersion

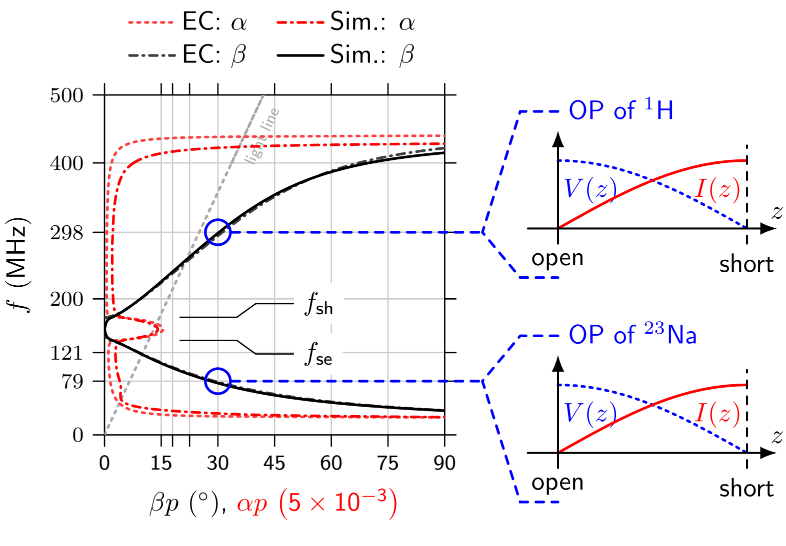

Figure 3. Dispersion diagram (left) of the periodic structure calculated on one hand with the equivalent circuit of Fig. 2 and on the other hand obtained by an FDTD simulation of the 3D structure. The desired principle current and voltage curves along the resulting quarter-wave resonator at the operating points (OP) are indicated on the right hand side.

was calculated on the basis of the equivalent circuit and on the other hand obtained with a full-wave FDTD simulation in EMPIRE-XPU of a CRLH TL followed by a recalculation to the unit cell using ABCD parameters. It is worth noting that the given equivalent circuit predicts the dispersion of the considered unit cell very well, which is particularly useful for rapid designs.

The final structure of the quarter-wave CDRA consists of a CRLH TL covering three unit cells and is terminated with a short circuit at one end whereas the other end is terminated with an open circuit. Feeding takes place at the open circuit and requires a dual-tuned matching network as presented in [5]. The CDRA element has the total dimensions of $21\,\mathrm{cm} \times 9\,\mathrm{cm} \times 2\,\mathrm{cm}$, which renders it a very compact dual-tuned RF-coil for multi-channel MRI applications.

3. Full-wave simulations and measurement results

The CDRA prototype was first numerically evaluated using EMPIRE-XPU. A phantom filled with body tissue simulating liquid (BTSL) with $\epsilon_\mathrm{r} = 61.8$ and $\sigma = 0.804\,\mathrm{S\,m^{-1}}$ was placed 20 mm above the CDRA and is modelled as a half-space. The results of the simulations are shown in Fig. 4, where a centered longitudinal slice displays the magnitude of the $\boldsymbol{B}_1$-field normalized to the square root of the accepted power together with the magnitude of the current density of the strip conductor. The latter consists of the sum of the current densities on both the upper and lower metal parts (MIM structure on the RO3010 substrate) which is visualized as a warped surface on top of the CDRA. Additionally, the integral current along the strip conductor is

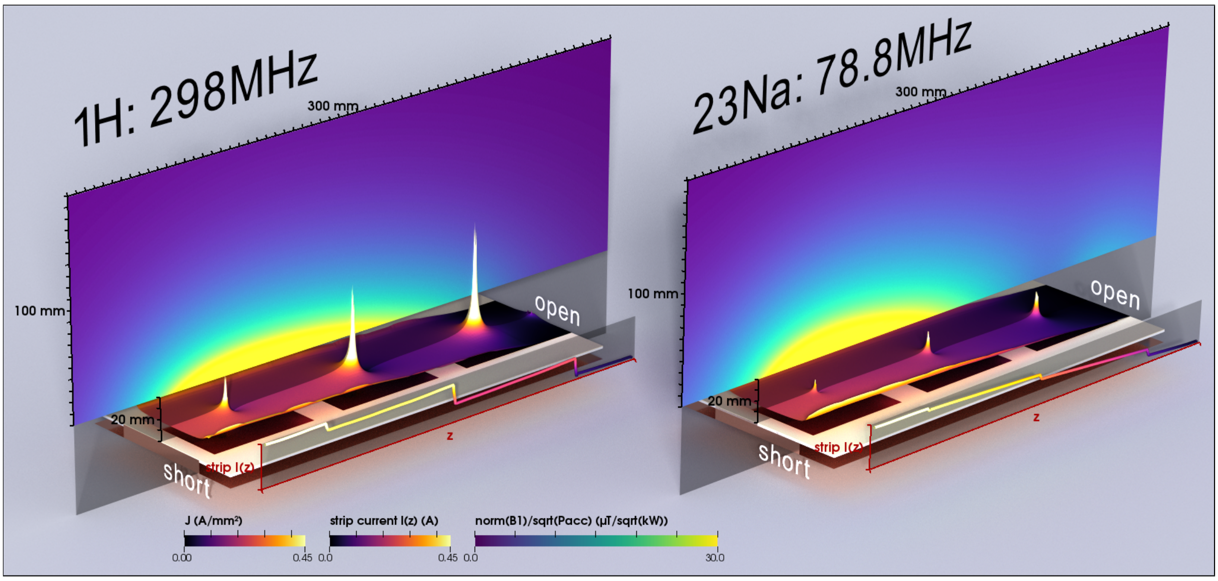

Figure 4. FDTD simulation results (EMPIRE-XPU) are visualized with ParaView. For both operating frequencies of the CDRA the normalized $\boldsymbol{B}_1$-field distribution is shown in a centered longitudinal slice. Additionally, the current density of the strip conductor is visualized as a warped surface above the CDRA, whereas the total current through the strip conductor is shown as a curve along the z-axes.

shown as a curve and indicates (along with the other field visualizations) very well the quarter-wave resonance behavior at the two operating frequencies. However, a staircase like sinusoidal approximation is obtained in the current curve at the low frequency, which is caused by the quite high phase shift along the unit cell, but shows no significant effect on the distribution of the $\boldsymbol{B}_1$-field inside of the phantom.

An initial MR experiment with two CDRA prototypes was carried out at the Erwin L. Hahn institute (Essen, Germany). The obtained MR images are given in Fig. 5 for the ^{23}Na nuclei

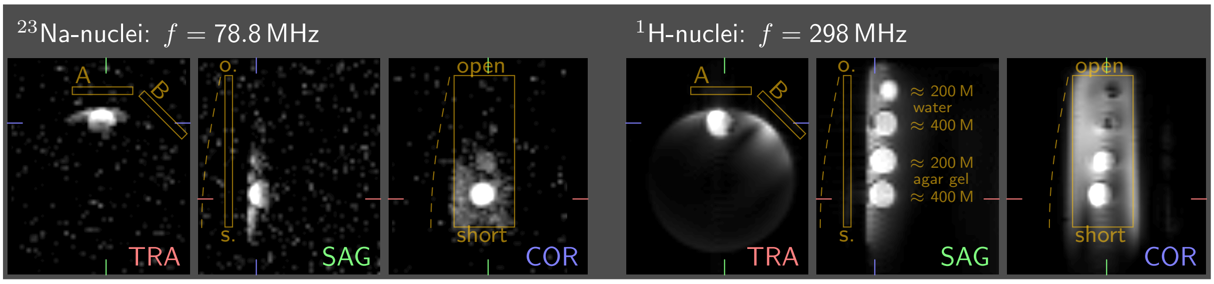

Figure 5. Initial MR images with two quarter-wave CDRAs where coil A is used for TX/RX and coil B for RX only [4]. The utilized phantom is a plastic canister with a diameter of about 20 cm It is filled with BTSL and contains additional ping-pong-ball insets filled with water salt or agar gel salt BTSLs of high sodium concentrations. The concentrations are indicated in the sagittal (SAG) hydrogen image. [Utilized sequence: 3D-gradient-echo, $T_R = 50$ ms, $T_E = 2$ ms, FoV: 244 mm × 300 mm × 300 mm, slice thickness of 4.70 mm, 4 sample average]

on the left hand side as well as for the ^{1}H nuclei on the right hand side. A plastic canister with a diameter of 20 cm and a height of about 35 cm filled up with BTSL composed of a water sugar salt solution and additionally containing four differently filled ping-pong ball insets was used as a phantom for the measurement. The ping-pong ball insets are filled with BTSLs either based on water salt solutions or agar-water-salt gels, but all having high sodium concentrations of 200 M or 400 M simulating diseased cartilage tissue.

The results are showing that the desired operating principle is successfully demonstrated but with a quite low SNR in case of the sodium-based images. Near the maximum of the $\boldsymbol{B}_1$-field and therefore near the maximum of the current density of the strip conductor (cf. Fig. 4) the best image quality is observed. Due to the quarter-wave field distributions only the balls filled with agar gel are visible, whereas the one with the lower sodium concentration can barely be seen. The images based on the hydrogen nuclei are of good quality but taken with a low resolution for comparison.

4. Conclusion

A dual-tuned coil element is presented providing quarter-wave resonance behavior at the two operating frequencies of the ^{23}Na- and ^{1}H nuclei for combined 7 T-MRI. The initial MR images prove the applicability of the proposed CDRA concept which yields very compact coil elements apt to be scaled-up to a flexible multi-channel coil system.

5. Acknowledgements

The authors would like to thank Harald H. Quick, Oliver Kraff and Stephan Orzada of the Erwin L. Hahn Institute (Essen, Germany), for their support and help at the 7 T–MRI scanner.

References

[1] Thulborn K R 2018 *NeuroImage* **168** 250–268 ISSN 1053-8119

[2] Haneder S and Konstandin S 2016 *Radiol.* **56** 159–169 ISSN 1432-2102

[3] Caloz C and Itoh T 2006 *Electromagnetic Metamaterials: Transmission Line Theory and Microwave Applications: The Engineering Approach* (Hoboken, NJ, USA: John Wiley & Sons, Inc.) ISBN 978-0-471-66985-2

[4] Svejda J T, Rennings A and Erni D 2017 *Tm - Tech. Mess.* **84** 2–12 ISSN 0171-8096

[5] Svejda J T, Erni D and Rennings A 2016 *2016 German Microwave Conference (GeMiC)* (Ratingen, DE: IMATech e.V.) pp 104–107 ISBN 978-3-9812668-7-0